Journal of Power Sources 189 (2009) 378–384

Contents lists available at ScienceDirect

Journal of Power Sources

journal homepage: www.elsevier.com/locate/jpowsour

Ni sulfide/$Ti_{50}Ni_{50}$ electrode with the superelasticity

K.W. Bae[a], H.S. Kim[a], G.B. Cho[a], K.W. Kim[a], K.K. Cho[a], J.H. Lee[b], T.H. Nam[a,*]

[a] School of Materials Science and Engineering & ERI, Gyeongsang National University, 900 Gajwa-dong, Jinju, Gyeongnam 660-701, Republic of Korea
[b] Department of Materials Science and Engineering, Donga University, Republic of Korea

ARTICLE INFO

Article history:
Received 8 July 2008
Accepted 7 August 2008
Available online 15 August 2008

Keywords:
Flexible battery
Ni sulfides
$Ti_{50}Ni_{50}$ alloy
Superelasticity
Electrochemical properties

ABSTRACT

Ni sulfides layers were formed on the surface of a $Ti_{50}Ni_{50}$ alloy by reacting sulfur with a Ni film deposited on the alloy, and then microstructures, transformation behavior, shape memory characteristics, superelasticity and electrochemical properties were investigated. When a Ni film deposited on a $Ti_{50}Ni_{50}$ alloy was annealed under the sulfur pressure of 100 kPa at 623 K, sulfides layers consisted of NiS and NiS_2 were formed. When annealing was made at 648 K with annealing time less than 0.9 ks, sulfides layers with a mixture of NiS and NiS_2 were formed, while only NiS_2 was formed when it was made for 1.8 ks. When annealing was made at 673 K with annealing time longer than 0.9 ks, only NiS_2 was formed. With raising annealing temperature and prolong annealing time, NiS changed into NiS_2 accompanied with a morphological change from a particulate-like to a dense film-like. A $Ti_{50}Ni_{50}$ alloy with surface NiS_2 layer showed the two-stage B2–R–B19′ transformation behavior, the shape memory effect and a partial superelasticity with a superelastic recovery ratio of 78%. NiS_2 cathode showed a clear discharge behavior with multi-voltage plateaus induced by intermediate reaction products; NiS and Ni_3S_2. The initial discharge capacity was 743 mA h g^{-1} corresponding to 85% of theoretical capacity and 65% of capacity duration is obtained at 20th discharge.

1. Introduction

Recently flexible electronic devices such as display, electronic paper (E-paper) and keyboard have been developed for next generation personal computers (PCs). Those devices essentially require flexible power sources (batteries) that can be flexible together with them. Flexible secondary batteries are recognized to be necessary for many portable electrical appliances, such as a wearable computer because they are heading for small system and multifunction [1–3].

Usually, secondary batteries are consisted of active materials, electrode, electrolyte and current collectors. In order to obtain a flexible secondary battery, its constituents should be flexible. As for electrodes, many kinds of materials such as graphite, Li-oxides, sulfides are adopted.

Metal sulfides such as Co, Cr, Cu, Mn, Ti, V, Ni sulfides have been studied as cathode materials because of their high energy density [4,5]. Among them, Ni sulfide has been of great interest because of its high capacity and good cycle characteristics [6–9]. Those electrode materials usually are used in the form of powders and pasted on current collectors with polymer binders. Electrolyte materials are usually used in the form of liquid or solid. In case of solid electrolyte, polymer materials with high flexibility are usually used. Therefore, electrode materials and electrolytes are not considered to be detrimental to the flexibility of batteries.

As for current collector materials, aluminum and nickel are currently used because of their high corrosion resistance and low electrical resistance. They are considered to be detrimental to the flexibility of secondary batteries because they show only small elastic strain less than 0.2%. Therefore, new current collector materials should be developed for realizing highly flexible secondary batteries. Ti–Ni alloys are regarded to be good candidates for current collector materials of a flexible secondary battery because they show the superelasticity, high corrosion resistance and proper electrical resistance. The superelasticity in Ti–Ni alloys have been known to be originated from the thermo-elastic martensitic transformation [10]. Thermo-mechanical treatments and aging have been adopted for improving the superelasticity of Ti–Ni alloys [11–14]. Recently there has been an attempt to apply Ti–Ni alloys for current collector materials of secondary batteries [15]. From the study, it was concluded that superelastic Ti–Ni alloys are comparable to Al as a current collector material.

In addition to the superelasticity, Ti–Ni alloys were found to be convenient for fabricating electrodes. Ti sulfides and Ni sulfides are easily formed on the surface of Ti–Ni alloys by annealing under sulfur atmosphere [16,17]. In the new electrode, Ti and Ni sulfides

* Corresponding author. Tel.: +82 55 751 5307; fax: +82 55 751 1749.
E-mail address: tahynam@gsnu.ac.kr (T.H. Nam).

0378-7753/$ – see front matter © 2008 Elsevier B.V. All rights reserved.
doi:10.1016/j.jpowsour.2008.08.012

act as cathodes and Ti–Ni substrate act as a current collector. The electrode showed the superelasticity and a clear charge–discharge behavior [16]. The new flexible secondary battery showed multi-voltage plateau due to the fact that cathode was a mixture of Ti and Ni sulfides [17]. In general, a single voltage plateau is desirable for applications.

In this study, Ni thin film was deposited on Ti–Ni current collectors, and then annealed under sulfur atmosphere in order to obtain only Ni sulfides. Purpose of the present study is to fabricate a superelastic Ni sulfides/Ti–Ni electrode, and then to investigate microstructure, transformation behavior, electrochemical properties and superelasticity of the electrode.

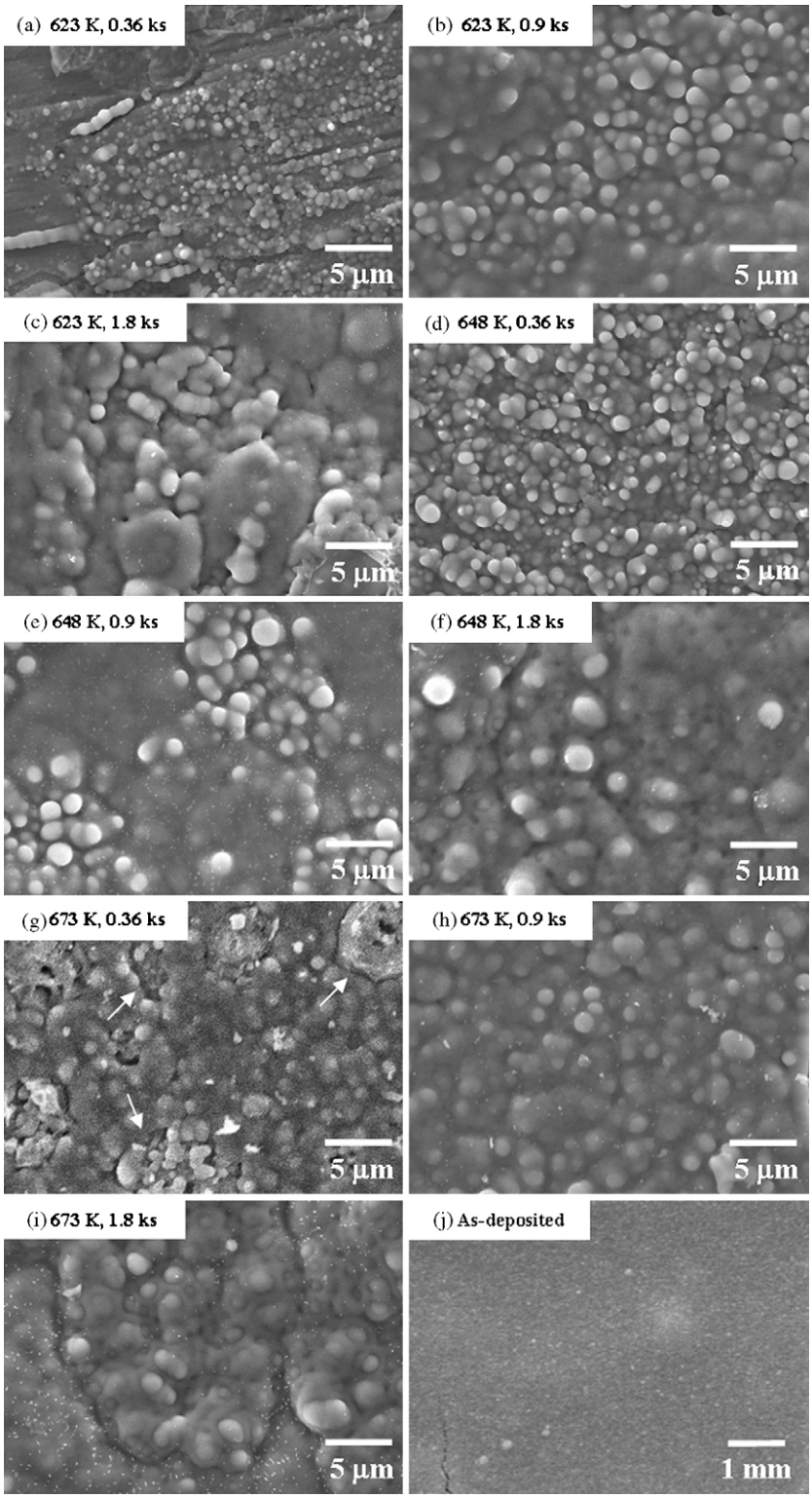

Fig. 1. SEM micrographs of sulfide layers formed under various annealing conditions. SEM micrograph of as-deposited Ni film on TiNi substrate is presented in (j).

2. Experimental procedure

A $Ti_{50}Ni_{50}$ alloy ingot was prepared by vacuum induction melting and then hot rolled into a sheet. After hot rolling, the sheet was cold rolled with a final cold working ratio of 35%. All specimens cut from the cold rolled sheet were annealed at 673 K for 3.6 ks in vacuum. After heat treatment, specimens were mechanically polished in order to remove oxide films, and then they were cleaned using acetone and methyl alcohol. A Ni film was deposited on the $Ti_{50}Ni_{50}$ substrate with DC magnetron sputtering. Sputtering was made at the pressure of less than 2.4×10^{-2} Torr and Ar gas of 300 sccm was flowed into a chamber. After the Ni deposition, specimens were put into a silica tube of 15 mm diameter with sulfur and then sealed in vacuum. The vacuum sealed ampoules were isothermally annealed in the temperature range of 623–673 K for 0.36–1.8 ks. The sulfur pressure inside the ampoules was 100 kPa.

Microstructure of specimens was observed using scanning electron microscope (SEM). In order to investigate the crystal structure of sulfides formed on the surface of $Ti_{50}Ni_{50}$ substrate, X-ray diffraction (XRD) experiments were made using Cu Kα radiation with a scanning rate of $2^\circ\,min^{-1}$. Transformation behavior of specimens was investigated by differential scanning calorimetry (DSC) measurements with a cooling and heating rate of $0.17\,K\,s^{-1}$. The shape memory characteristics were investigated by thermal cycling tests under constant load with a cooling and heating rate of $0.017\,K\,s^{-1}$. Elongation on cooling and its recovery on heating were measured by linear variable differential transformer. The superelasticity was examined by tensile tests at various temperatures with a strain rate of $10^{-4}\,s^{-1}$.

Li/sulfides cells were assembled in stainless steel cell holders and then galvanostatic discharge–charge test was performed at constant current. Li foil was used as an anode and sulfides formed on a $Ti_{50}Ni_{50}$ current collector were used as a cathode. 1 M $LiCF_3SO_3$ in tetraethylenglycol dimethylether (TEGDME) was used as an electrolyte. The rest time before discharging was 4 h, where open circuit voltage (OCV) was stabilized for cells. The current density was $87.1\,mA\,g^{-1}$ corresponding to 0.1 C rate. Mass of active material was calculated from density (NiS_2: $4.00\,g\,cm^{-1}$).

3. Results and discussion

3.1. Microstructures of Ni sulfide/$Ti_{50}Ni_{50}$ electrode

Fig. 1 shows SEM micrographs of surfaces of sulfide layers formed on a $Ti_{50}Ni_{50}$ substrate. Sulfide layers were formed by annealing Ni film deposited on a Ti–Ni substrate at 623–673 K for 0.36–1.8 ks under the sulfur pressure of 100 kPa. For comparison, a SEM micrograph of surface of Ni film before annealing is shown in Fig. 1(j). Surface of Ni film deposited on TiNi alloy seems to be smooth and flat. By annealing the Ni film at 623 K for 0.36 ks, spherical particles are formed as seen from Fig. 1(a). With raising annealing temperature from 623 to 648 K, the particles are found to grow (compare Fig. 1(a) with (d)). With further raising annealing temperature from 648 to 673 K, a dense film-like layer is formed above the particles as shown by arrows in Fig. 1(g). Similar film-like layer is formed when annealing time is longer than 0.9 ks at 623 and 648 K. This suggests that two kinds of sulfide layers are formed, one is particulate-like layer and the other is film-like layer, depending on annealing temperature and annealing time.

Cross-sectional SEM micrographs of sulfide layers are shown in Fig. 2. Specimens were prepared by fracturing a part of sulfide layer. For comparison, a cross-sectional of the Ni film deposited on a $Ti_{50}Ni_{50}$ substrate is shown in Fig. 2(d). Thickness of the as-deposited Ni film is found to be about 0.5 μm. In the specimen annealed at 648 K for 0.36 ks (Fig. 2(a)), a particulate-like sulfide layer with a thickness of about 1–2 μm is observed. With prolonging annealing time from 0.36 to 0.9 ks, a dense film-like sulfide layer is formed on the particulate-like layer with a thickness of about 3.2 μm as shown in Fig. 2(b). In the specimen annealed at 673 K for 1.8 ks (Fig. 2(c)), only a dense film-like layer with a thickness of about 5 μm is observed. Comparing Fig. 2(a)–(c), it is found that thickness of sulfide layer increases with increasing annealing temperature and time.

In order to characterize surface layers in Fig. 1, X-ray diffraction experiments were made on the specimens, and then X-ray diffraction patterns obtained are shown in Fig. 3. For comparison, X-ray diffraction pattern of the Ni film deposited on a $Ti_{50}Ni_{50}$ substrate is shown in Fig. 3(j). In Fig. 3(j), diffraction peaks corresponding to

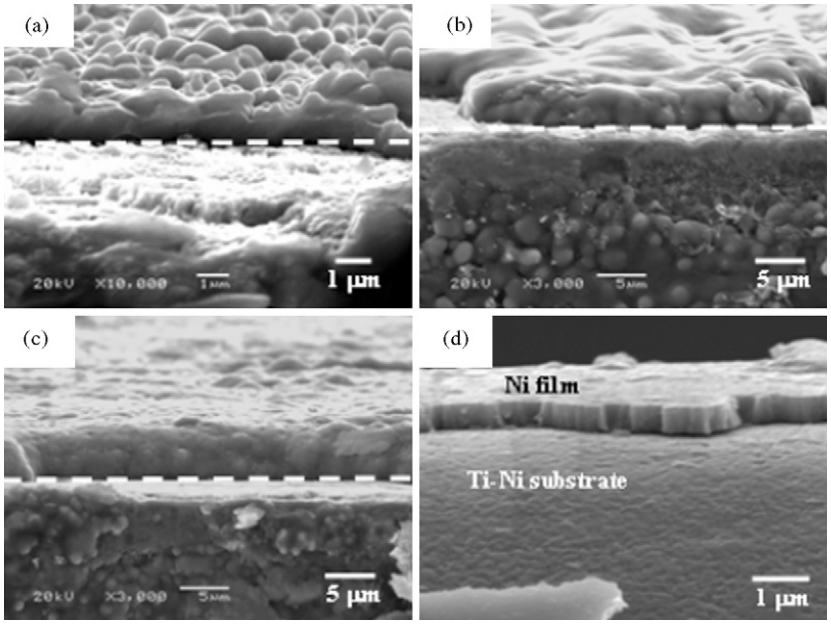

Fig. 2. Cross-sectional SEM micrographs of sulfide layers formed under various annealing conditions of (a) 648 K, 0.36 ks, (b) 648 K, 0.9 ks and (c) 673 K, 1.8 ks. Cross-sectional SEM micrograph of as-deposited Ni film deposited on TiNi substrate is presented in (d).

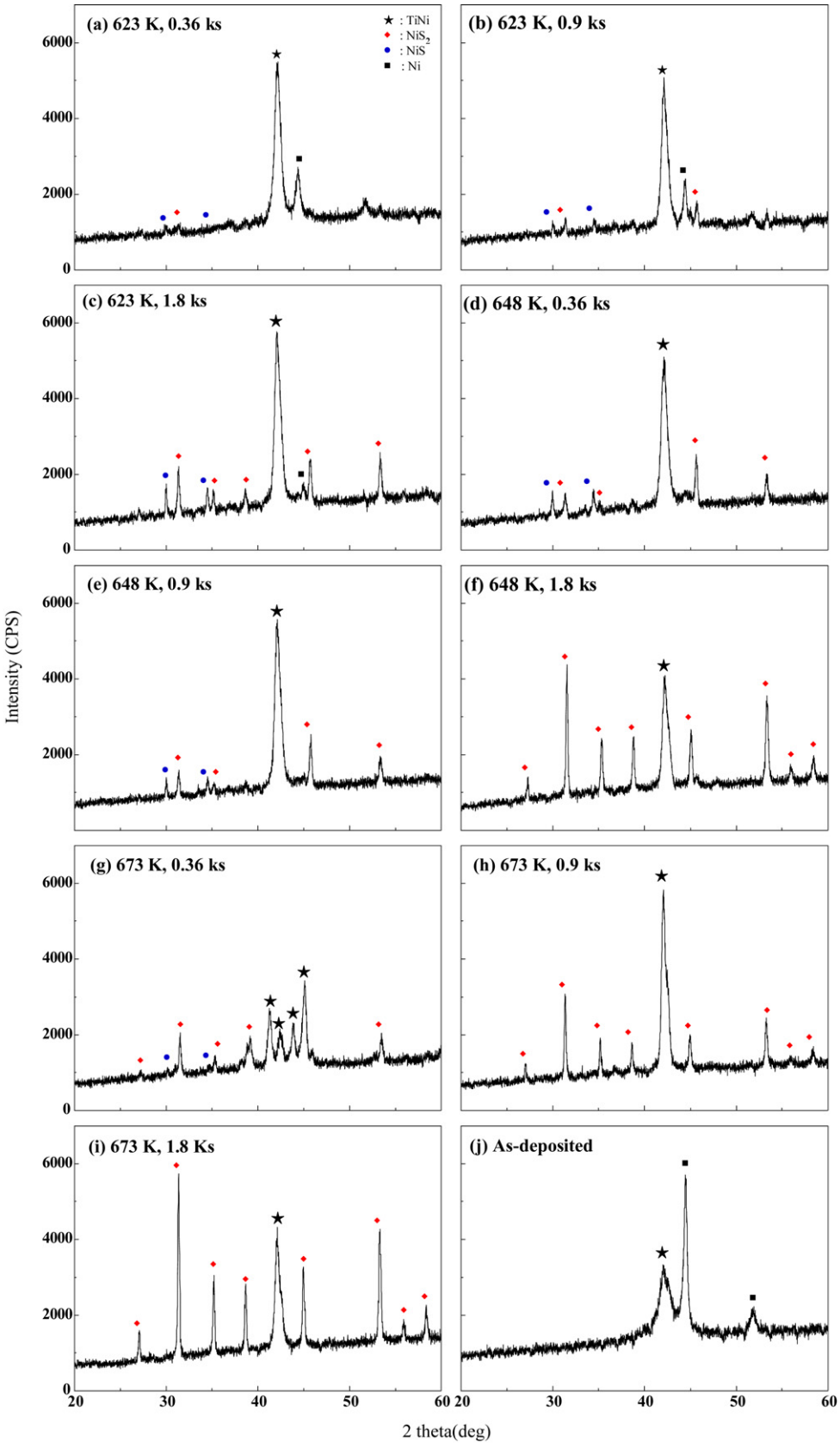

Fig. 3. X-ray diffraction patterns of sulfides formed obtained various annealing conditions. X-ray diffraction pattern of as-deposited Ni film on TiNi substrate is presented in (j).

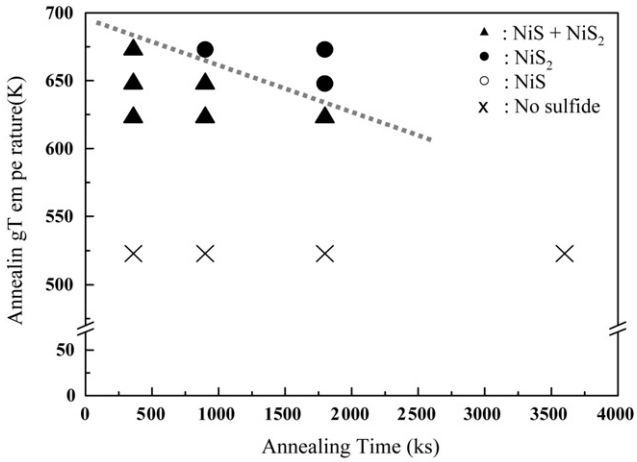

Fig. 4. Phase diagram of Ni sulfides as functions of annealing temperature and annealing time.

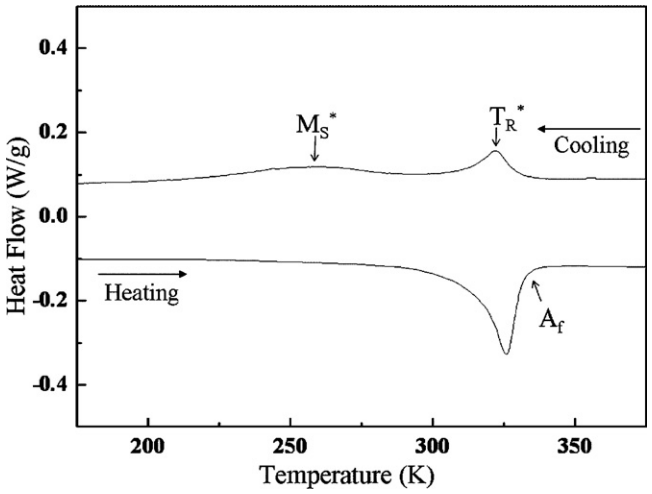

Fig. 5. DSC curves of specimens annealed at 673 K for 1.8 ks.

$Ti_{50}Ni_{50}$ substrate with B2 structure [10] and Ni are observed. In the specimens annealed at 623 K for 0.36 ks and 623 K for 0.9 ks, weak diffraction peak corresponding to NiS and NiS_2 are observed in addition to those of $Ti_{50}Ni_{50}$ substrate and Ni film. Therefore, the spherical particles observed in Fig. 1(a) are known to be NiS. On prolonging annealing time from 0.36 to 0.9 ks, strong diffraction peaks corresponding to NiS_2 are observed (Fig. 3(b)), and the dense film-like layer covering the particulate-like layer in Fig. 1(b) is known to be NiS_2. On further prolonging annealing time, intensity of diffraction peaks corresponding to NiS and NiS_2 increases as shown in Fig. 3(c).

In the specimens annealed at 648 K for 0.36 ks, diffraction peaks corresponding to NiS and NiS_2 are found in addition to those of $Ti_{50}Ni_{50}$ substrate and Ni film (Fig. 3(d)). On prolonging annealing time, intensity of diffraction peaks corresponding to NiS and NiS_2 increases as shown in Fig. 3(d). In the pattern of Fig. 3(d), a diffraction peak corresponding to Ni is not observed, which means that all Ni film reacted with sulfur. On further increasing annealing time, diffraction peaks of NiS are not observed while intensity of those of NiS_2 increases (Fig. 3(f)), which means that NiS changes into NiS_2 with increasing annealing time. In the specimens annealed at 673 K for 0.36 ks, diffraction peaks corresponding to NiS and NiS_2 are found in addition to those of $Ti_{50}Ni_{50}$ substrate (Fig. 3(g)). On prolonging annealing time, diffraction peaks of NiS are not observed while intensity of those of NiS_2 increases (Fig. 3(h)). On further increasing annealing time, intensity of diffraction peaks of NiS_2 increases (Fig. 3(i)). A phase diagram of Ni sulfides obtained from Fig. 3 is shown in Fig. 4. It is found that stability of NiS_2 increases with increasing annealing temperature and time. Any sulfides were not observed in the specimens annealed at 523 K.

3.2. Superelasticity and shape memory effect of Ni sulfide/$Ti_{50}Ni_{50}$ electrode

Fig. 5 shows DSC curve of the specimen annealed at 673 K for 1.8 ks under sulfur atmosphere. This specimen has NiS_2 sulfide layer with a thickness of 5 μm on the surface of Ti–Ni substrate as shown in Figs. 2 and 3. Two DSC peaks are found on the cooling curve, while only one DSC peak is observed on the heating curve. The peak designated by T_R^* is due to the B2–R transformation, and that designated by M_s^* is due to the R–B19′ transformation. The DSC peak on heating curve is ascribed to the B19′–B2 reverse transformation. Similar transformation behavior has been reported in thermo-mechanically treated Ti–Ni alloys [18,19]. This suggests that surface of Ni sulfides does not affect transformation behavior of a $Ti_{50}Ni_{50}$ alloy.

In order to investigate the superelasticity and shape memory effect of the specimen annealed at 673 K for 1.8 ks, tensile tests were made at various temperatures, and then stress–strain curves obtained are shown in Fig. 6. In the stress–strain curves obtained at 285, 305 and 325 K which are lower than A_f (the B19′–B2 reverse transformation finish temperature), most of strain developed on loading is recovered on heating up to 373 K after unloading. This means that the specimen annealed at 673 K for 1.8 ks under sulfur atmosphere shows the shape memory effect. In the curve obtained at 330 K (A_f), strain developed on loading is partly recovered on unloading. This means that the specimen annealed at 673 K for 1.8 ks under sulfur atmosphere shows a partial superelasticity. The superelastic recovery ratio defined as $(A/B) \times 100$ is measured to be 78% from Fig. 6(d), which is some lower than that of thermo-mechanically treated Ti–Ni alloys (~100%). The partial superelasticity is ascribed to NiS_2 sulfide layer formed on Ti–Ni substrate. From Fig. 6, it is concluded that the specimen annealed at 673 K for 1.8 ks under sulfur atmosphere shows the shape memory effect and partial superelasticity.

3.3. Electrochemical properties of Ni sulfide/$Ti_{50}Ni_{50}$ electrode

Specimen annealed at 673 K for 1.8 ks, where only NiS_2 sulfide layer was observed as shown in Figs. 2 and 3, was used to investigate its electrochemical properties. Fig. 7 shows initial charge–discharge curves of a cell with NiS_2 electrode. Two voltage plateaus (1.57 and 1.40 V) are observed in the first discharge curve while there are three plateaus (1.86, 1.68 and 1.40 V) in the second discharge curve. The low voltage plateau in the first discharge curve is ascribed to the high surface resistance of dense NiS_2 layer as shown in Fig. 1(i). Such the discharge behavior was also observed in other cells with specimens annealed at the same condition (not shown here). Thus it is found that the charge–discharge reaction is stabilized after the first charging. Three-step reaction occurs in NiS_2 electrode fabricated in this work, indicating that various reaction products are reversely composed and decomposed during discharge–charge process.

In order to clarify the reaction products during discharge, electrode obtained at 1.7 V of cut-off voltage (A in Fig. 7) were analyzed by TEM. The reason why cut-off voltage of 1.7 V is selected is to trace intermediate Ni sulfides. Before the TEM observation, the electrodes obtained after the second discharge were dried in a vacuum chamber for 7 days. Fig. 8 shows TEM image obtained from a piece

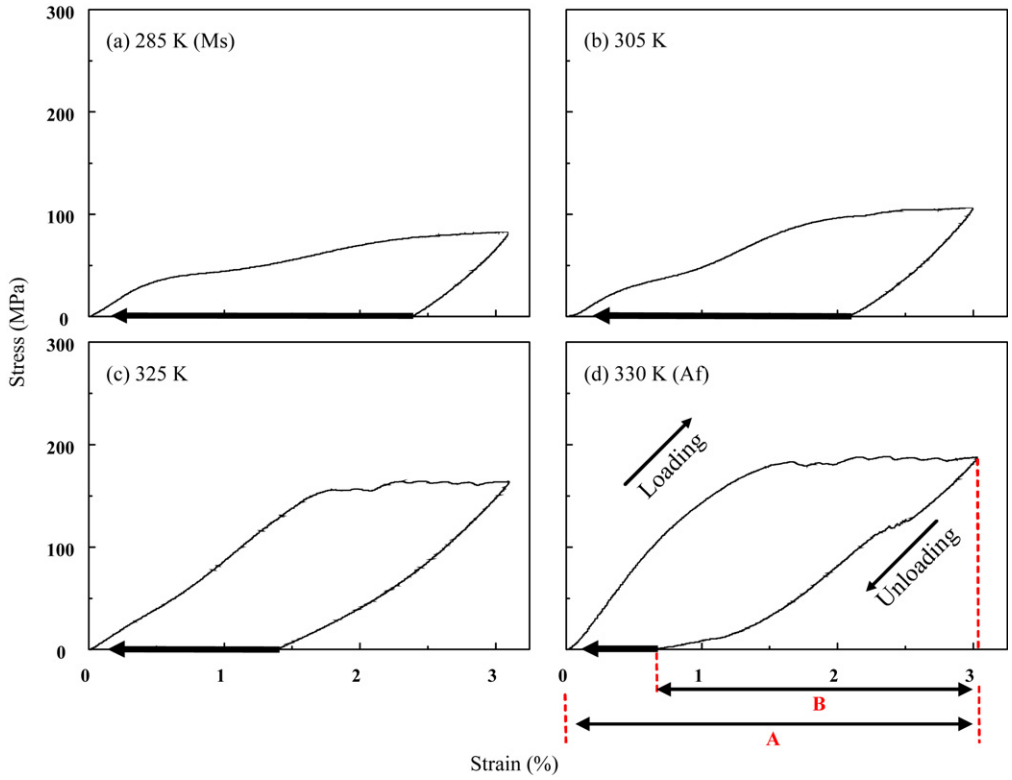

Fig. 6. Stress vs. strain curves of specimen annealed at 673 K for 1.8 ks. Curves were obtained at various test temperatures of (a) 285 K, (b) 305 K, (c) 325 K and (d) 330 K.

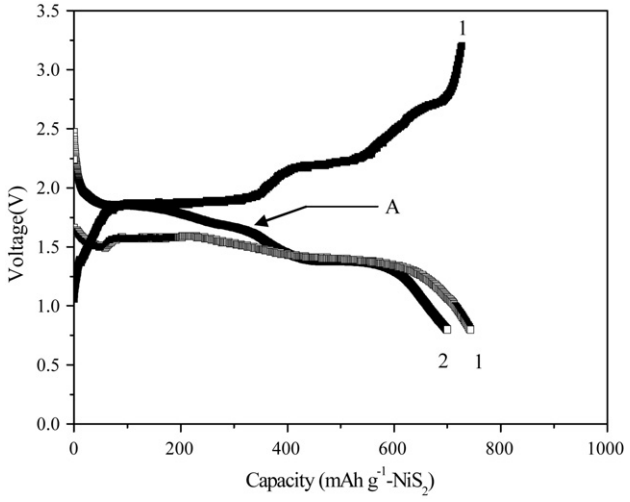

Fig. 7. Initial charge–discharge curves of cell with NiS_2/TiNi electrode prepared by annealing at 673 K for 1.8 ks. Cycling number is presented in curve.

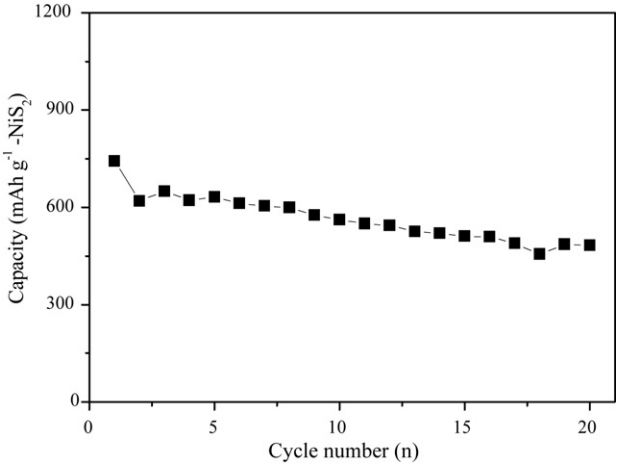

Fig. 9. Cycle performance of cell with NiS_2/TiNi electrode prepared by annealing at 673 K for 1.8 ks.

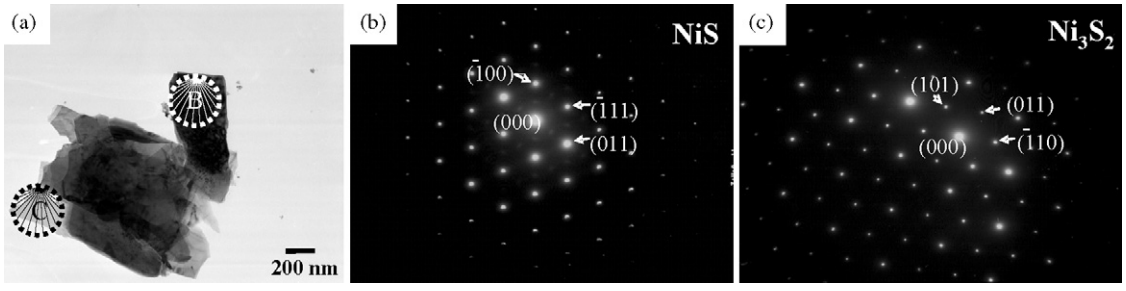

Fig. 8. Electron diffraction patterns of discharged electrodes with cut-off voltages of (a) 1.75 V and (b) 1.50 V.

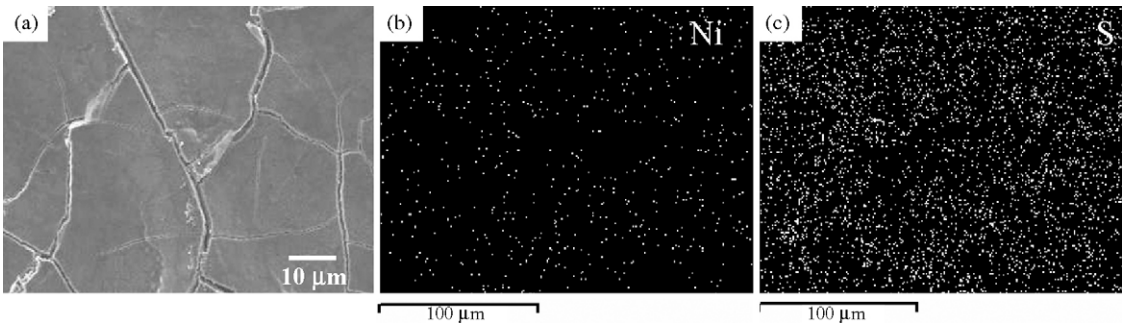

Fig. 10. SEM photograph and EDS mapping images of electrode obtained after 15th discharge. EDS mapping images correspond to elements of (b) Ni and (c) S.

of electrodes and electron diffraction patterns obtained from area *B* and *C* in (a). From analysis of patterns, discharge products at 1.7 V are known to be NiS and Ni_3S_2. This means that initial NiS_2 changes to NiS and Ni_3S_2 during discharge process. No significant difference in morphology of two sulfides could be found. Detecting Li_2S which exists in electrode was difficult due to high activity in air. Therefore, it is believed that NiS_2 shows a sequential change in a series of sulfides from NiS_2 to NiS, to Ni_3S_2 and finally to Ni, and all the reactions are accompanied with the formation of Li_2S. This result shows a good agreement with reaction voltages between Li and Ni sulfides [17].

The discharge capacity vs. cycle number plot of cell with NiS_2 electrode annealed at 673 K for 1.8 ks is presented in Fig. 9. The initial discharge capacity is 743 mA h g^{-1} corresponding to 85% of theoretical capacity (871 mA h g^{-1}). Discharge capacity abruptly decreases at the first cycle and dull capacity fading is observed from the second cycle. 65% of capacity duration is obtained after 20 cycles. The good cycle performance is resulted from the formation of well adhesive NiS_2 layer on TiNi current collector, which can be proved by good mechanical properties as mentioned above. Moreover, the good adhesion of NiS_2 electrode could be confirmed through surface observation.

Surface of $NiS_2/Ti_{50}Ni_{50}$ electrode obtained after 15th discharge was investigated by SEM and EDS, and then results obtained are shown in Fig. 10. Even though cracks which may occur during cyclic charge–discharge procedure are observed on the surface, layers are well stuck on TiNi current collector. Elements of Ni and S are detected from EDS mapping as shown in Fig. 10(b) and (c). Relatively large amount of S exists on the surface compared to Ni. This suggests that electrode surface consists of Ni and Li_2S as final products.

4. Conclusions

Ni sulfides were formed by reacting sulfur with Ni film deposited on a $Ti_{50}Ni_{50}$ alloy, and then microstructures, martensitic transformation behavior, shape memory characteristics, superelasticity and electrochemical properties were investigated. Results obtained are as follows:

(1) When Ni film deposited on a $Ti_{50}Ni_{50}$ alloy was annealed at 623 K, Ni sulfides layers consisted of NiS and NiS_2 were formed. At 648 K annealing, when annealing time was less than 0.9 ks, Ni sulfides layers with a mixture of NiS and NiS_2 were formed, while only NiS_2 was formed when the annealing time is 1.8 ks. At 673 K annealing, only NiS_2 was formed when the annealing time is longer than 0.9 ks.

(2) With increasing annealing temperature and time, NiS changed into NiS_2 with a morphological change from a particulate-like to a dense film-like.

(3) A $Ti_{50}Ni_{50}$ alloy with surface NiS_2 layer showed the two-stage B2–R–B19′ transformation behavior on cooling and the one-stage B19′–B2 on heating.

(4) A $Ti_{50}Ni_{50}$ alloy with surface NiS_2 layer showed the shape memory effect and partial superelasticity with a superelastic recovery ratio of 78%.

(5) NiS_2 sulfide electrode formed on the Ti–Ni current collector showed a clear discharge behavior with multivoltage plateaus, which was ascribed to intermediate electrochemical reactions during $4Li + NiS_2 \leftrightarrow Ni + 2Li_2S$.

(6) The initial discharge capacity of Ni sulfides formed on the Ti–Ni current collector was 743 mA h g^{-1} corresponding to 85% of theoretical capacity and 65% of capacity duration was obtained at 20th discharge.

Acknowledgement

This work was supported by University IT Research Center Project in Gyeongsang National University.

References

[1] F. Susan, S. John, A. Cristina, G. Levent, P. Fritz, S. Daniel, S. Asim, W. Lee, Comput. Aided Des. 28 (1996) 393.
[2] R. Lin, J.G. Kreifeldt, Int. J. Ind. Ergon. 27 (2001) 259.
[3] J.F. Knight, C. Baber, Appl. Ergon. 38 (2007) 237.
[4] E. Peled, D. Golodnitsky, E. Strauss, J. Lang, Y. Lavi, Electrochim. Acta 43 (1998) 1593.
[5] R.A.J. Sharma, J. Electrochem. Soc. 123 (1976) 448.
[6] R. Jasinski, B. Burrows, J. Electrochem. Soc. 116 (1969) 422.
[7] A. Olivias, J. Cruz-Reyes, V. Petranovskii, M. Avalos, J.S. Fuentes, J. Vac. Sci. Technol. A 16 (1998) 3515.
[8] S.C. Han, H.S. Kim, M.S. Song, S. Paul Lee, J.Y. Lee, H.J. Ahn, J. Alloys Compd. 349 (2003) 290.
[9] S.C. Han, H.S. Kim, M.S. Song, J.H. Kim, H.J. Ahn, J.Y. Lee, J. Alloys Compd. 351 (2003) 273.
[10] W.J. Buehler, J.W. Gilfrich, R.C. Wiley, J. Appl. Phys. 34 (1963) 1473.
[11] S. Miyazaki, K. Otsuka, Philos. Mag. A 50 (1984) 393.
[12] S. Miyazaki, Y. Ohmi, K. Otsuka, Y. Suzuki, J. Phys. 43 (1982) C4–255.
[13] M. Nishida, T. Honma, J. Phys. 43 (1982) C4–75.
[14] T. Saburi, T. Tatsumi, S. Nenno, J. Phys. 43 (1982) C4–261.
[15] G.B. Cho, S.S. Jeong, S.M. Park, T.H. Nam, Mater. Sci. Forum 486–487 (2005) 650.
[16] G.B. Cho, K.W. Kim, H.J. Ahn, K.K. Cho, T.H. Nam, J. Alloys Compd. 449 (2008) 308.
[17] H.S. Kim, J.S. Kim, M.K. Kim, K.K. Cho, T.H. Nam, J. Power Sources 178 (2008) 758.
[18] V.N. Khachin, V.E. Gjunter, V.P. Sivokha, A.S. Savvinov, Proceedings of ICOMAT-79, Boston, 1979, p. 474.
[19] T. Todoroki, H. Tamura, J. Jpn. Inst. Met. 50 (1986) 538.